A combined modeling and measurement approach to assess the nodal tide modulation in the North Sea

Robert Hagen[1], Andreas Plüß[1], Leon Jänicke[2], Janina Freund[1], Jürgen Jensen[2] and Frank Kösters[1]

[1]Federal waterways engineering and research institute Hamburg, Germany
[2]Research Institute for Water and Environment

Key Points:

- Nodal modulation can be extracted from tide records through multiple, non-linear fitting of annually analyzed tidal constituents.
- Theoretical nodal modulation, derived from the equilibrium tide theory, does not apply consistently in the North Sea.
- Friction causes the generation of shallow water tides, which influence the nodal modulation of lunar constituents and S_2 significantly.

Corresponding author: Robert Hagen, `robert.hagen@baw.de`

Abstract

The correct representation of the 18.61 year nodal tide is essential for an interpretation of the evolution of mean sea level, as errors cause misleading bias. The nodal tide is currently estimated by applying correction factors in harmonic analysis, which are derived from the equilibrium tide. From the equilibrium tide, correction values f for amplitude and u for phase are determined, which alter lunar tidal constituents, depending on the nodal cycle. This approach has proven to be valid for many tide gauges, even though the impact of the nodal tide in shelf seas has been shown to differ from their theoretical correction value. Hence, tidal constituents from tide records in the North Atlantic shelf region were analyzed for their nodal amplitude and phase lag with a new multiple, non-linear regression approach, which is able to approximate the nodal modulation quantitatively and its agreement to the theoretical equilibrium tide. Results show an overestimation of the lunar M_2 and N_2 constituents by the equilibrium of more than 2.7% in the Wadden Sea, while O_1 and K_2 are underestimated by 1 to 4.6%, which would produce an error of 2 to 5 cm e.g. in the German Wadden Sea. Additionally, a process-based model of the North Sea was applied at the diurnal minimum and maximum of the nodal cycle to calculate the spatial distribution of f and u. Model results reproduce a regionally varying pattern of f and u, indicating how the amplitude modulation of nodal constituents in shallow areas is distributed.

Plain Language Summary

The nodal tide is a part of the tidal regime, which changes the tidal range on a reoccurring timescale of 18.61 years, originating from the gravitational force of the moon. A nodal amplitude can be up to 30 cm, which makes its accurate consideration essential for the analysis of sea level rise. In current studies, the influence of the nodal tide is approximated percentage-wise, as its reoccurrence interval is too long for conventional analysis. This study has found, based on 31 tide records in the European North Sea, that current analysis methods are inaccurate in the Northern English Channel and the Wadden Sea by several centimeters based on the influence of the nodal tide. This is analyzed with a new method, which uses statistical methods to approximate the nodal tide from measured tide records. We conclude that the inaccurate estimate is restricted to shallow and geometrically complex parts of the North Sea. As most tide gauges are located near the coast in shallow water, these findings may have major implications on the correct approximation of the mean sea level (MSL).

1 Introduction

The scientific assessment of past and future mean sea level (MSL) trends requires reliable predictions of natural cyclic behavior on short and long time scales. Typical cycles concerning sea level are tides, which are a result of the gravitational potential of sun and moon, centrifugal force of the earth and meteorological forcing. Tides are distinguished by their frequency, which is predominantly diurnal or semidiurnal, even though monthly, interannual, annual and perennial frequencies exist as well. The nodal tide (Bradley, 1728) is a harmonic signal with a period of 18.61 years, caused by the precession of the lunar ascending node (Pugh, 1987). It is the most important low frequency tidal constituent apart from the lunar perigee and it has shown to have an amplitude of up to 30 cm (Peng et al., 2019). In order to consider the nodal tide in MSL analysis, the theoretical equilibrium tide concept is applied (Proudman, 1960; Godin, 1986; Woodworth, 2012). Non-resolved low frequency cyclic behavior of water levels may lead to an erroneous estimation of sea level rise (SLR). The influence of the nodal cycle variations on the tidal potential of e.g. M_2 is assumed to be 3.7 % on global average (Haigh et al., 2011) or 2.2 cm in global mean amplitude (Baart et al., 2012). However, local effects of the nodal cycle can vary significantly and the greatest values occur in diurnal regions with tidal ranges of ≥ 4 m (Haigh et al., 2011). Spatial variations occur not only due to variable water depths but also due to non-linear frictional, tidal-tide interactions (Ku et al., 1985), changing energy propagation or/ dissipation and other non-linear effects (Jay et al., 2015). The magnitude and spatial dependence of these changes already make it evident that the nodal cycle cannot be neglected for water level analysis based on tide gauge data, as it would cause a bias. Pugh (1987) also emphasized that the nodal cycle is significant, but difficult to separate for MSL determinations. Therefore, the nodal component of a lunar constituent must either be eliminated or equalized by considering only full nodal periods. This applies not only to tidal analysis but to MSL studies and tidal high and low water level analyses as well, especially when trends are estimated (Jensen et al., 1988, 1992). The Dutch coast is an example for this, where a non-consideration of the nodal cycle conceals the changes in MSL (Baart et al., 2012). This necessity occurs not only in reconstructions, but also in projections. In the case of reconstructions, a correction is necessary for both tidal analyses and MSL determinations from gauge data in order to obtain unbiased results.

Even though long tide records do exist today, a reliable detection of the nodal tide signal remains difficult, e.g. due to data quality limitations, noise (Rossiter, 1967; Trupin & Wahr, 1990) or overlying trends (Woodworth & Blackman, 2004; Woodworth et al., 1991). The commonly applied correction for the nodal tide in harmonic analysis (e.g. UTide by Codiga (2011)) is based on assumptions from the equilibrium tide theory (Pugh, 1987). Tidal constituent amplitudes from harmonic analysis are modulated by a percentage-wise adjustment (f, i.e. nodal modulation) and a nodal phase lag (u), respectively. These correction parameters are considered to be globally constant (Trupin & Wahr, 1990; Woodworth, 2012). The consideration of the nodal modulation (also nodal satellite variation Haigh et al. (2011)) in amplitude and phase is therefore performed by applying the stationary correction parameters f and u (also $f-u$ correction following Pugh (1987)) to lunar, tidal constituents. Nodal amplitudes and phase lags, as well as nodal satellite variation, have been investigated globally (Cherniawsky et al., 2010; Menéndez & Woodworth, 2010) and regionally e.g. in the North Sea (Amin, 1985; Hansen et al., 2015; Jensen et al., 1992; Woodworth et al., 1991), the Gulf of Maine (Ray, 2006), the Mediterranean Sea (Shaw & Tsimplis, 2010), the Chinese Sea (Feng et al., 2015) and the western coast of Australia (Amin, 1993) to name only a few. Evaluations of the $f-u$ correction parameters have been published by Cherniawsky et al. (2010), who carried out a harmonic analysis of satellite sea surface elevation data to determine nodal satellites. Their analyzed nodal amplitudes overestimated the equilibrium tide parameters f and u, especially when dealing with small amplitudes. Contrary to this, an analysis of tidal constituents in the Chinese seas has shown an underestimation of the nodal modulation parameters for M_2 and N_2, while O_1 and K_1 agree well with the theoretical values (Feng et al., 2015). In the Mediterranean Sea, the nodal variation agrees well overall with the equilibrium assumption (Shaw &

Tsimplis, 2010). Hence, many findings either challenge or agree with the statements from Trupin and Wahr (1990), who stated that the amplitude and phase are close to their equilibrium amplitude and phase. However, it must be noted, that regional exceptions, e.g. for the North Sea, were made in their results.

Thus, as the nodal modulation does not follow the equilibrium tide theory consistently across all coastal waters, the first major aim of this study is to develop a method to quantify the nodal satellite variation, i.e. nodal correction parameters f and u, from tide records. We use a multiple, non-linear regression approach to calculate the nodal modulation at gauges in the European North Sea from tidal constituents, before comparing them to the equilibrium value. The second goal of this study is the identification and description of the processes causing the deviation from equilibrium modulation. In order to assess the spatial distribution for f and u, numerical simulations are carried out. In fact, Woodworth (2012) already suggested a barotropic approach for 19 consecutive years without explicit loading as a way to advance the topic of the accuracy of the current nodal correction formulation. In this study, we deploy a three-dimensional, astronomically forced, numerical model of the North Sea at the diurnal minimum and maximum of nodal modulation in order to obtain spatial distributions through differences. These results provide detailed, spatial information about the regional nodal modulation and phase lag. Based on these results, a recommendation on how to consider nodal satellite variation in the future can be made, which is the third major aim of this study.

This paper is organized as follows: The applied data and the preprocessing are discussed in the first part from Section 2.1 to 2.3. Afterwards a brief description of the numerical model and its validation are given in Section 2.4. Section 3.1 to 3.4 describe the results from the multiple non-linear regression fitting approach, before the outcome of the numerical simulations is described in Section 3.5. Results are interpreted and discussed in Section 4.

2 Material and methods

2.1 Nodal Tide Modulation

Modern harmonic tidal analyses extract amplitude and phase of tidal constituents, defined by given astronomical frequencies, from tide records. The astronomical frequencies (i.e. tidal constituents) are defined by their lunar or solar origin and their reoccurance interval, hence the semidiurnal moon tide is called M_2. The harmonic analysis (i.e. satellite method) follows the development of tidal potential theory (Doodson, 1921, 1928) and is well documented with its modern formulations (Foreman et al., 2009; Godin, 1972; Pugh, 1987). Tidal constituents underlie interannual, annual and perennial fluctuations, which have an influence on the results of a harmonic analysis (Feng et al., 2015; Gräwe et al., 2014; Hansen et al., 2015; Müller et al., 2014). In this study, we will focus on fluctuations with an interannual frequency. These are most prominently represented by the nodal tide (18.61 years) and the lunar perigee (8.85 years), while the solar perigee is negligible for practical applications due to its long timescale of 20,392 years. For a full review on the scientific background to the nodal tide and the lunar perigee we recommend Haigh et al. (2011). In order to consider the nodal tide variation, tidal constituents are modified in harmonic analysis based correction parameters from the equilibrium tide theory (Pugh, 1987). The modulation effect amounts to an amplitude adjustment of 3.7 % or phase lag of -2.1 ° for the M_2 or 28.6 % and -17.7 ° for K_2 constituent for example. This correction procedure is referred to as $f-u$ correction. Since tidal records are typically analyzed for less than a full nodal cycle in practice, tidal constituents are corrected for the nodal variation within a harmonic analysis. However, the $f-u$ satellite correction (i.e. Table 1 following Pugh (1987)) assumes that nodal modulation always follows the equilibrium tide theory, which is valid for most gauges (Trupin & Wahr, 1990), but has been shown to be inappropriate locally, especially in shelf seas.

Table 1: Nodal correction parameters f (amplitude) and u (phase) derived from the equilibrium tide. N is the longitude of the moon's ascending node in ° with 0 ° being the time at which diurnal terms are at a maximum, e.g. in November, 1987 or June 2006.

	f (amplitude)	u (phase)
M_m	$1.000 - 0.130\ cos(N)$	0.0 °
M_f	$1.043 + 0.414\ cos(N)$	$-23.7\ °\ sin(N)$
$Q_1,\ O_1$	$1.009 + 0.187\ cos(N)$	$10.8\ °\ sin(N)$
K_1	$1.006 + 0.115\ cos(N)$	$-8.9\ °\ sin(N)$
$M_2,\ N_2$	$1.000 - 0.037\ cos(N)$	$-2.1\ °\ sin(N)$
K_2	$1.024 + 0.286\ cos(N)$	$-17.7\ °\ sin(N)$

Table 1 lists the correction values f and u for lunar tidal constituents. Note that the amplitude and phase lag are maximal for the diurnal constituents at $N = 0°$ for M_f, Q_1, O_1, K_1 and K_2, which would be in June 2006, and for M_2, N_2 at $N = 180$ ° which would be e.g. in October 2015. Thus, if one imagines an exemplary mean amplitude of 1 m for M_2, the $f-u$ correction procedure would correct M_2 in June 2006 (minimum) to 0.963 m and in October 2015 (maximum) to 1.037 m, giving M_2 a nodal amplitude of 0.037 m. If K_2 had a mean amplitude of 1 m, its amplitude would be 1.286 m in June 2006 and 0.714 m in October 2015.

2.2 Tide Records

This study utilizes 31 North Sea and North Atlantic tide records from Germany, Great Britain, France, the Netherlands and Denmark as a data basis for harmonic analysis. Figure 1 lists all gauges and the period of valid data hereinafter. The longest tide records are located in Brest, France (1845-2019), Delfzijl, the Netherlands (1879-2019), Esbjerg, Denmark (1889-2015), Newlyn, Great Britain (1915-2016) and Cuxhaven, Germany (1918-2018). Most Dutch and British tidal records start in the 1970s, while the German measurements start predominately in the late 1990s. The data was carefully controlled by visual inspection, checked for anomalies and harmonized to equidistant hourly values, as required for harmonic analyses (Codiga, 2011). Otherwise, tide records remain unchanged, thus they were not cleared from MSL trend, surge or noise. In order to determine the nodal component, a time series of at least 19 years is required and we define, in accordance with Peng et al. (2019), a minimum completeness of at least 60 % valid hourly entries for each year and tide record for further analysis.

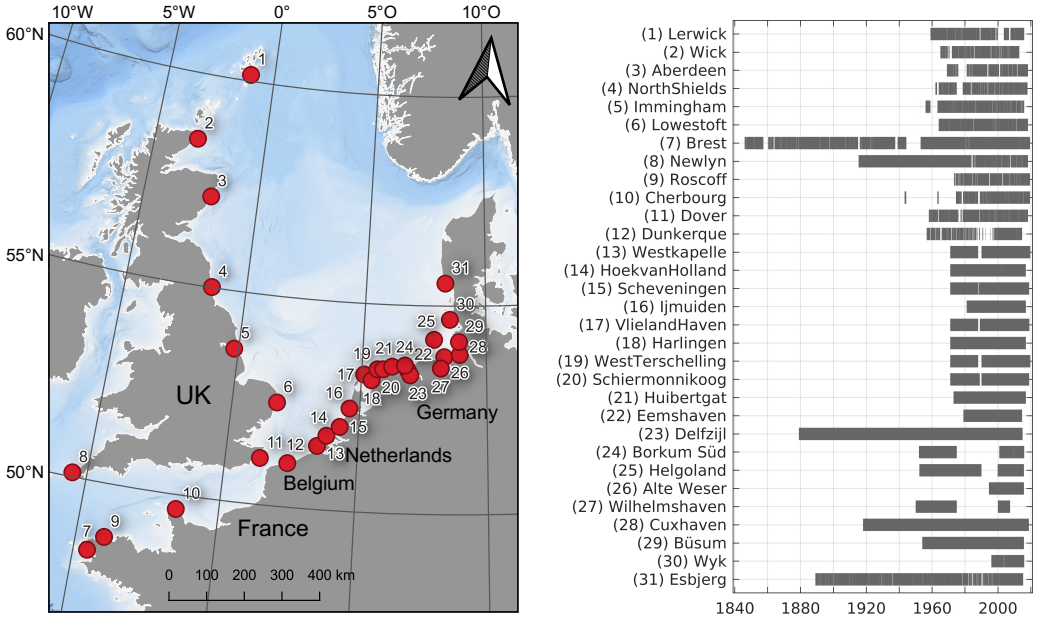

Figure 1: Tide records used in this study in the northern Atlantic and the North Sea from 1846 to 2019 with a temporal resolution of 1 hour. The data is arranged in the direction of the propagation of the Kelvin wave (counterclockwise) in the North Sea (Lerwick to Lowestoft), the English Channel (Brest to Ijmuiden) and the Dutch and German Wadden Sea (Vlieland Haven to Esbjerg).

2.3 Nodal Tide Fitting

In literature, different techniques are applied to extract the nodal tide from water level signals. Most recently, the quantile fitting method (Woodworth & Blackman, 2004) was applied to gauges worldwide showing clear nodal signals in 371 of 527 gauges (Peng et al., 2019) in the 90 % quantile. The harmonic analysis for the nodal constituents has also been carried out globally (Cherniawsky et al., 2010), using a 16 year long satellite altimetry data set. Additionally, multiple non-linear regressions of annual tidal characteristic values (Jensen et al., 1988, 1992; Woodworth et al., 1991), mean sea level (Baart et al., 2012; Hansen et al., 2015) and tidal constituents (Feng et al., 2015; Shaw & Tsimplis,

2010) was conducted to obtain information about the amplitude and phase of the nodal tide.

The results of the quantile method for tidal characteristic values or their percentiles as well as water level quantiles in the western English Channel and the Wadden Sea were inconclusive in this study, as neither nodal nor lunar perigee signal could be detected. We suspect that frequent wind and storm surge events as well as strong shallow water effects deform the signals and limit the applicability of the quantile analysis method. Thus, the nodal modulation model is applied to tidal constituents. The model is a non-linear, least square fitting approach shown in Equation 1 (Feng et al., 2015; Jensen et al., 1992; Peng et al., 2019) including an acceleration trend term (Baart et al., 2012). We chose an annual analysis period (January to December) for a reliable estimation of "true" (Pugh, 1987) tidal constituents and to minimize the effect of interannual variation of partial tides in shelf seas (Gräwe et al., 2014; Menéndez & Woodworth, 2010; Müller et al., 2014).

In Equation 1 the parameter a_0 denotes the initial sea level, a_1 accounts for the linear and a_2 for an accelerated trend with a time lag φ_1. The nodal tide term is represented by the amplitude a_3, the nodal frequency ω and a phase lag φ_2. The variable t represents the time in Julian years (365.25 d).

$$H(t) = a_0 + a_1 t + a_2(t - \varphi_1)^2 + a_3 \; sin(\omega t - \varphi_2)) \tag{1}$$

$$\omega = \frac{2\pi}{18.61}$$

To account for the rapid change in tidal constituents from the 1980s (Haigh et al., 2019; Müller, 2011) a time lag φ_1 has been added to the acceleration term a_2 (Baart et al., 2012; Houston & Dean, 2011). The goodness-of-fit between data and the non-linear model estimation is described by the coefficient of determination R^2. R^2 compares the dependence of two data sets with 1 being a perfect estimation. Following Peng et al. (2019) we chose results with a value of $R^2 \leq 0.5$ to be statistically insignificant in this study. Note, that fitting of the lunar perigee cycle was attempted by adding an additional term to Equation 1 analog to a_3 with a period of 4.4 years. However, results rarely produced statistical significance within the entire study area for the lunar perigee, which is consistent with previous results (Haigh et al., 2011; Menéndez & Woodworth, 2010). Whenever there was a satisfying agreement for the lunar perigee ($R^2 \geq 0.5$), its amplitude was more than 10 times smaller than the nodal amplitude. Therefore the lunar perigee has not been considered in the following.

2.4 Hydrodynamic Model

Even though the North Sea is monitored by one of the most closely meshed measurement networks worldwide (Sündermann & Pohlmann, 2011) information between tide gauges and far-off the coast is very limited. In order to close these gaps, this study deploys a numerical North Sea model, which is located on the European continental shelf in the northeastern Atlantic (Figure 2). The majority of the grid cells has been located within the German Bight and the Dutch Wadden Sea, as complex bathymetry with steep slopes and shallow embankments requires high grid resolution in order to reproduce realistic energy dissipation (Rasquin et al., 2020). 203.500 unstructured, horizontal elements have been used with an increasing grid resolution from typically 7.5 km in the open North Sea to 350 m in the Wadden Sea to less than 50 m in the estuaries of the German Bight.

The UnTRIM^2 model (Casulli & Walters, 2000) with the novel subgrid approach (Casulli, 2009) has been applied in order to consider complex bathymetry details at low computational cost. By applying a finer subgrid (increasing 4 to 12 times of the horizontal grid resolution) within the computational grid, the bathymetric information and therefore volume can be estimated with less effort than in conventional grids (Sehili et al., 2014). The hydrodynamic model has been thoroughly validated with measurements (Bundesanstalt für Wasserbau et al., 2019b) and the validation results from e.g. the year 2012 show a

root mean square error (RMSE) of 3.3 cm / 2.8 ° for the M_2, 1.1 cm / 4.1 ° for the S_2 and 0.7 cm / 3.5 ° for the N_2 tidal constituent, respectively. Water levels display a RMSE between 8 and 15 cm. The model uses a spatially varying bottom roughness, which has been calibrated to optimally fit the M_2 constituent.

In this study, the three dimensional, hydrodynamic model is applied with a clear focus on tidal dynamics. Other processes have not been considered (i.e. waves, salinity, temperature, sediments, surge and meteorology) in order to isolate the astronomical forcing entirely. Tidal constituents from the global tide model FES (FES2014 was produced by Noveltis, Legos and CLS and distributed by Aviso+, with support from Cnes (`https://www.aviso.altimetry.fr/`)) were reconstructed with ut_reconstr (Codiga, 2011) at the open boundary (blue line in Figure 2), using the default $f - u$ correction. The model bathymetry within the German Bight has been adapted from the EasyGSH-DB (`http://easygsh-db.org/`) project for the year 2006 (Bundesanstalt für Wasserbau et al., 2019a). Bathymetry for the Dutch Wadden Sea was obtained from Rijkwaterstaat, for the English coast from UKHO and for the French coast from SHOM. The remaining data gaps have been filled with data from the EMODnet database (EMODnet Bathymetry Consortium, 2016).

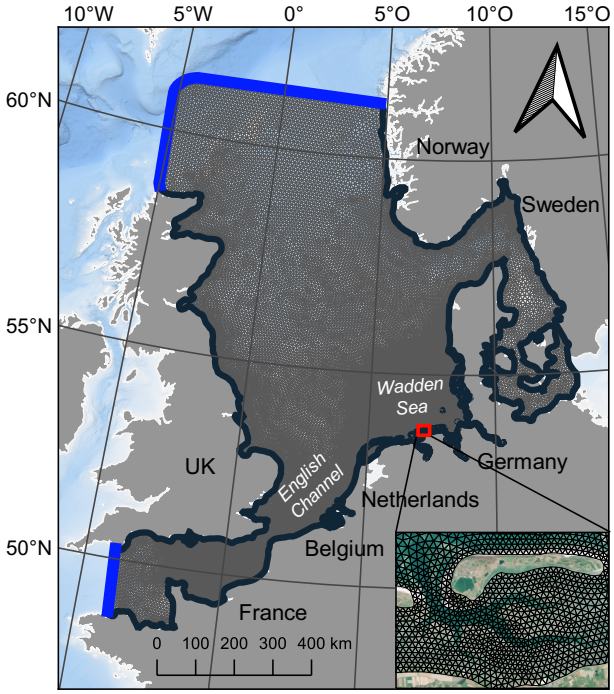

Figure 2: The study area North Sea, showing the grid lines in grey, the open boundary in blue and the closed boundary in black. The bottom right shows a representative grid resolution around the island of Norderney in Eastern Frisia, Germany.

3 Results

3.1 Fitting Evaluation

The dominant tidal constituents in the North Sea are the M_2, S_2, N_2, O_1, K_1 and K_2 components. In the following, the tidal constituents from measured tide gauge records given in Figure 1 are analyzed for their nodal amplitude modulation and phase lag using the fitting function from Equation 1. All harmonic analyses in the following are completed with the UTide algorithm (Codiga, 2011). UTide is applied using default settings with all tidal constituents available and without nodal correction.

The results of the analysis are shown in Figure 3 for two example locations, which have been chosen because of their different, geographical setting. Brest is located westwards from the North Sea in the north Atlantic Ocean while Büsum is placed within the German Bight near the Elbe and Eider estuary in the Wadden Sea. In order to quantify the goodness-of-fit, the R^2 has been calculated for each constituents nodal amplitude and phase lag in Brest and Büsum in Figure 4.

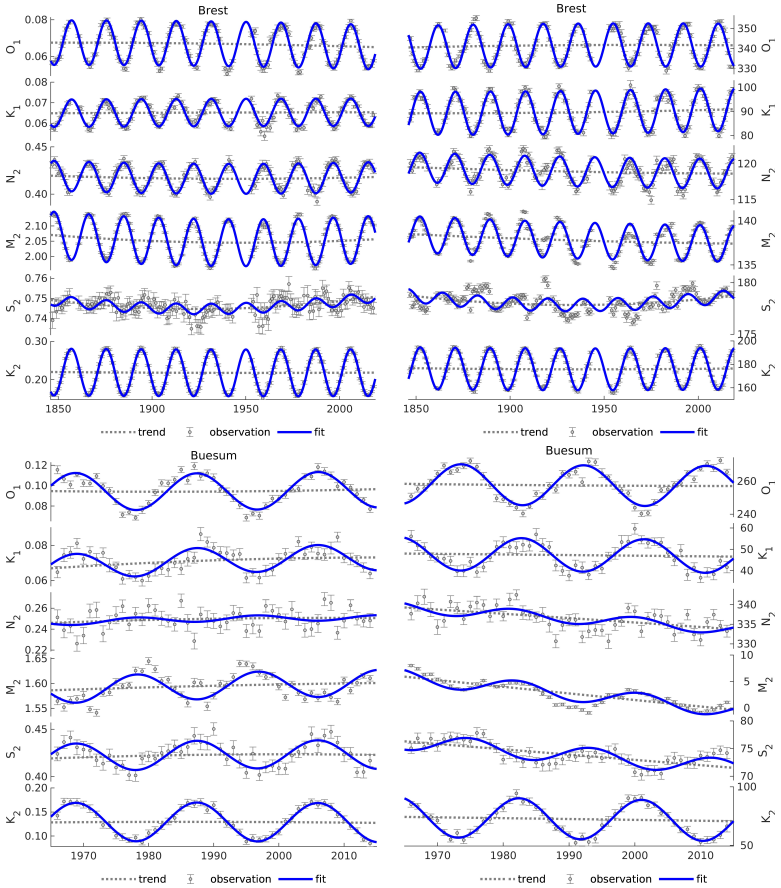

Figure 3: Fitting results for the tidal constituents M_2, S_2, N_2, O_1, K_1 and K_2 for Brest from 1846 - 2019 (top) and Büsum from 1954 - 2015 (bottom). The gray dots represent the resulting amplitude in m (left) and the phase in degree (right) of a harmonic annual analysis of water levels with their 95 % confidence interval from UTide. The dashed gray line indicates the linear and squared trend of the constituents, while the solid blue line represents the results of the multiple, non-linear regression fit.

The R^2 values indicate for Brest that the non-linear fitting method is reliable ($R^2 > 0.8$) for all constituents but S_2. In Büsum, the method yields only reliable results for O_1 and K_2 ($R^2 > 0.8$), while K_1, M_2 and S_2 are on the verge of statistical insignificance ($R^2 > 0.5$). However, visual inspection of the amplitude fitting of e.g. M_2 or K_1 in Figure 3 suggests agreement between the fitting approach and available data. In Brest, R^2 is usually between 0.05 to 0.25 higher, while phase and amplitude R^2 are comparable. The fitting of N_2 was unsuccessful in Büsum for phase and amplitude with a $R^2 < 0.5$.

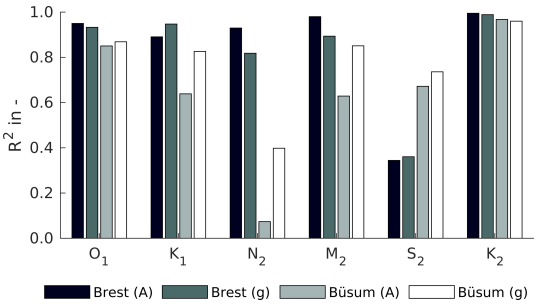

Figure 4: Coefficient of determination R^2 from the fitting for the tide records Brest and Büsum from Figure 3 with the function from Equation 1. A denotes the amplitude and g the phase of each tidal constituent.

The R^2 distribution from Figure 4 is extended to all stations and tidal constituents in Figure 5 below. The gauges have been sorted in the direction of the counterclockwise propagating Kelvin wave in the North Sea with a break in Lowestoft, where the tidal waves from Scotland (Lerwick to Lowestoft) and the English Channel (Brest to Ijmuiden) unite towards the Dutch and German Wadden Sea (Vlieland Haven to Esbjerg). In the following, as the agreement between phase and amplitude coincides at most gauges, their R^2 will be discussed together.

The index of agreement R^2 is consistently ≥ 0.85 at all locations for O_1 and K_2, showing that these constituents are steadily extractable from all tide records. M_2 also demonstrates high values for R^2 with several local exceptions such as the Dutch west coast in the northeastern English Channel (Hoek van Holland to Ijmuiden), West-Terschelling and Cuxhaven, whose R^2 is ≤ 0.5 for the amplitude modulation, even though the phase lag agrees well for all stations. For K_1, R^2 is between 0.6 and 0.93 with the exception of Dunkerque (0.5). K_1's R^2 diminishes in the English Channel from 0.83 in Cherbourg to 0.61 Dover before improving slightly in the north eastern English Channel near Hoek van Holland to a mean of 0.7. N_2 shows strong correlation (0.8 to 0.95) from Lerwick to Dover, before its R^2 decreases in the northern English Channel in Westkapelle near its amphidromical point, similar to M_2. Further eastwards, N_2 fitting remains inconclusive due to low statistical significance with the exception of Esbjerg where its nodal amplitude is lower than 0.5 cm. S_2 shows sufficient R^2 from the English Channel to the Wadden Sea, contrary to N_2. Nevertheless, low correlation ($R^2 \geq 0.5$) for S_2 can be seen for the amplitude in Lerwick to Dunkerque excluding Immingham, North Shields and Lowestoft. The phase of S_2 could not be fitted consistently, as R^2 is mostly ≤ 0.5, though slight phase modulation takes place in the Dutch and German Wadden Sea. The values for R^2 vary from 0.75 to 0.85 between Vlieland Haven and Büsum.

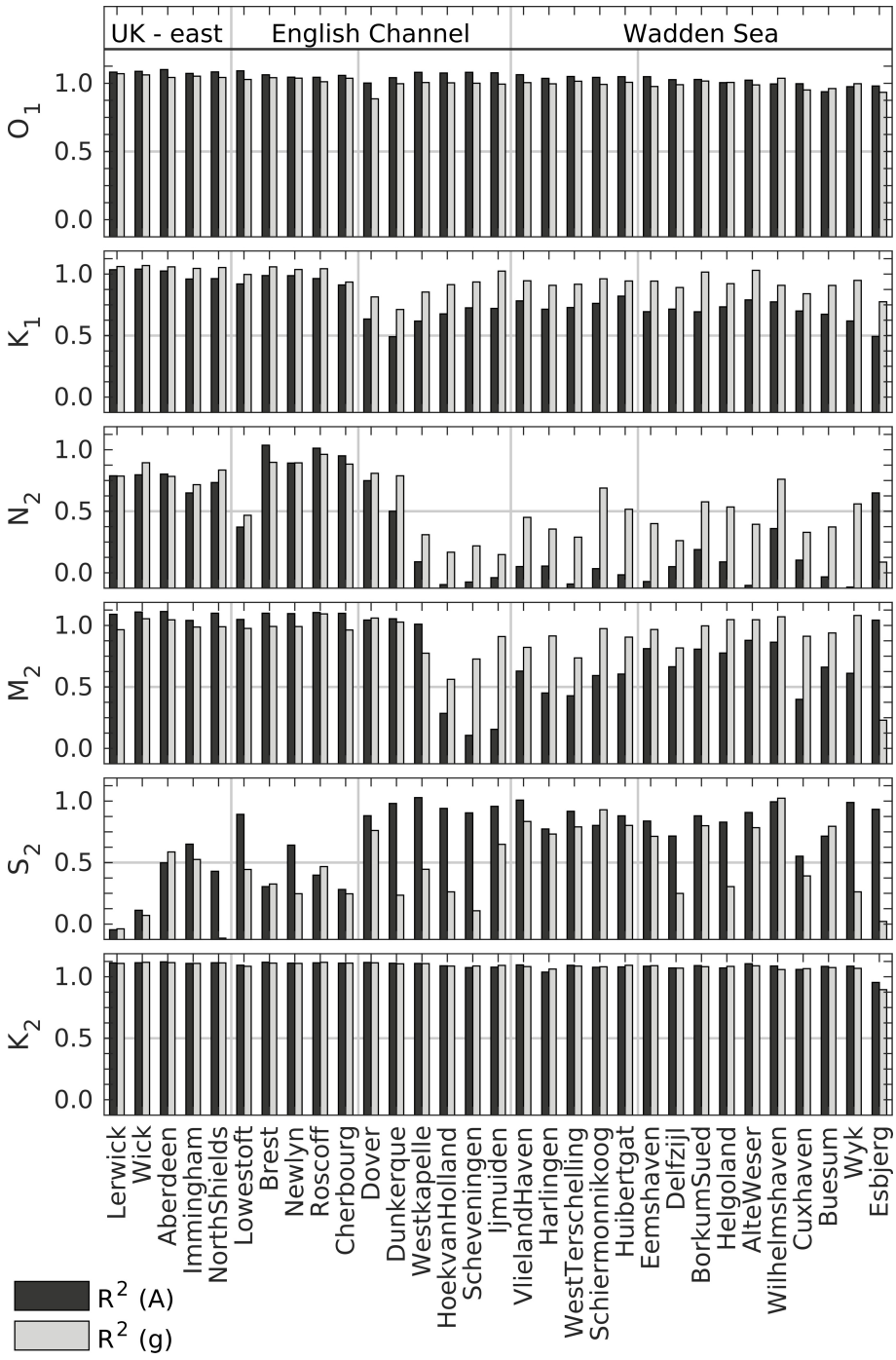

Figure 5: R^2 of amplitude and phase fitting as indicator for the goodness-of-fit of the multiple, non-linear regression approach for the components M_2, S_2, N_2, O_1, K_1 and K_2. R^2 for the amplitude (A) is drawn in black, while the results of the phase (g) fitting are represented in gray. The x-axis shows the tide record locations from Figure 1.

3.2 Seasonal Variation

Since tidal constituents underlie constant interannual variations (Gräwe et al., 2014; Müller et al., 2014), a sensitivity study is performed in order to quantify the effect of meteorological forcing on the estimation of nodal amplitudes with Equation 1. The method described with Equation 1 is now applied to all tide records in Table 2 for the constituent M_2 in the summer s (May to October) and winter w (November to April) half year as well as a full hydrological year a. In the following chapters, n denotes the nodal satellite of a tidal constituent. The chosen gauges represent a region in the North Sea study area. The English east coast (Aberdeen, Lowestoft), the English Channel (Brest, Roscoff, Dunkerque, Lowestoft), the Dutch Wadden Sea (Harlingen, Huibertgat) and the German Wadden Sea (Alte Weser, Büsum) are investigated for seasonal effects.

Table 2: Comparison between the summer and winter half-year to quantify the meteorological impact on the the non-linear, multiple regression fitting of nodal modulation from Section 2.3. s denotes summer, w winter, a the full hydrological year and n a nodal satellite. R^2 (coefficient of determination) is given in order to describe the goodness-of-fit for each scenario.

	$M_{2n,s}$ cm	$M_{2n,w}$ cm	$M_{2n,a}$ cm	$\frac{M_{2n,s}}{M_{2n,a}}$ $-$	$\frac{M_{2n,w}}{M_{2n,a}}$ $-$	${R^2}_s$ $-$	${R^2}_w$ $-$	${R^2}_a$ $-$
Aberdeen	3.7	3.5	3.5	1.06	1.00	0.98	0.75	0.94
Lowestoft	3.3	3.3	3.2	1.03	1.03	0.93	0.88	0.91
Brest	3.8	3.8	3.7	1.03	1.03	0.97	0.97	0.98
Roscoff	3.5	3.7	3.5	1.00	0.95	0.96	0.98	0.99
Dunkerque	2.4	2.6	2.4	1.00	1.08	0.91	0.91	0.94
Harlingen	1.5	1.5	1.3	1.15	1.15	0.54	0.60	0.60
Huibertgat	–	2.0	1.6	–	1.25	0.49	0.67	0.60
Alte Weser	1.5	1.7	1.4	1.07	0.82	0.75	0.59	0.82
Büsum	1.7	2.0	1.7	1.00	1.18	0.54	0.56	0.64

Results from Table 2 show, that the seasonal dependence of M_2's nodal modulation is always lower than $\pm$ 0.4 cm. The $M_{2n,s}$ and the $M_{2n,w}$ to $M_{2n,a}$ ratios deviate more from 1 with a low R^2 (≤ 0.75). The nodal satellite for M_2 at robust estimations, such as Aberdeen, Brest, Dunkerque or Roscoff, shows seasonal variation of less than 6 %, while weaker R^2, i.e. Harlingen, Huibertgat or Büsum produce an over- or underestimation in summer or winter by a maximum of 25 % of R^2. As seasonal variation in M_{2n}'s amplitude shows small variation, no bias due to seasonally heterogeneously sampled data is to be expected, when applying Equation 1. The analysis also shows, that R^2 is usually larger, after the analysis has been performed for an entire year. It is not surprising that we find the approximation of true tidal constituents to become more robust on a longer time timescale as this has already been stated by Pugh (1987).

3.3 Nodal Modulation at Gauges

After the nodal signal has been extracted successfully through multiple, non-linear regression fitting, its amplitude modulation f and phase lag u can be calculated from the regression parameters. If R^2 is ≤ 0.5, results have been regarded as statistically insignificant and will not be included in the subsequent analysis. Differences of the calculated modulation from the theoretical $f-u$ correction factors (i.e. Table 1) are given in Figure 6. Positive values represent an overestimation of the theoretical nodal correction factors f and u. For all constituents, the fitted nodal modulation and phase lag agree well with equilibrium

expectations at the English east coast (UK - east) and the southern English Channel (until Cherbourg).

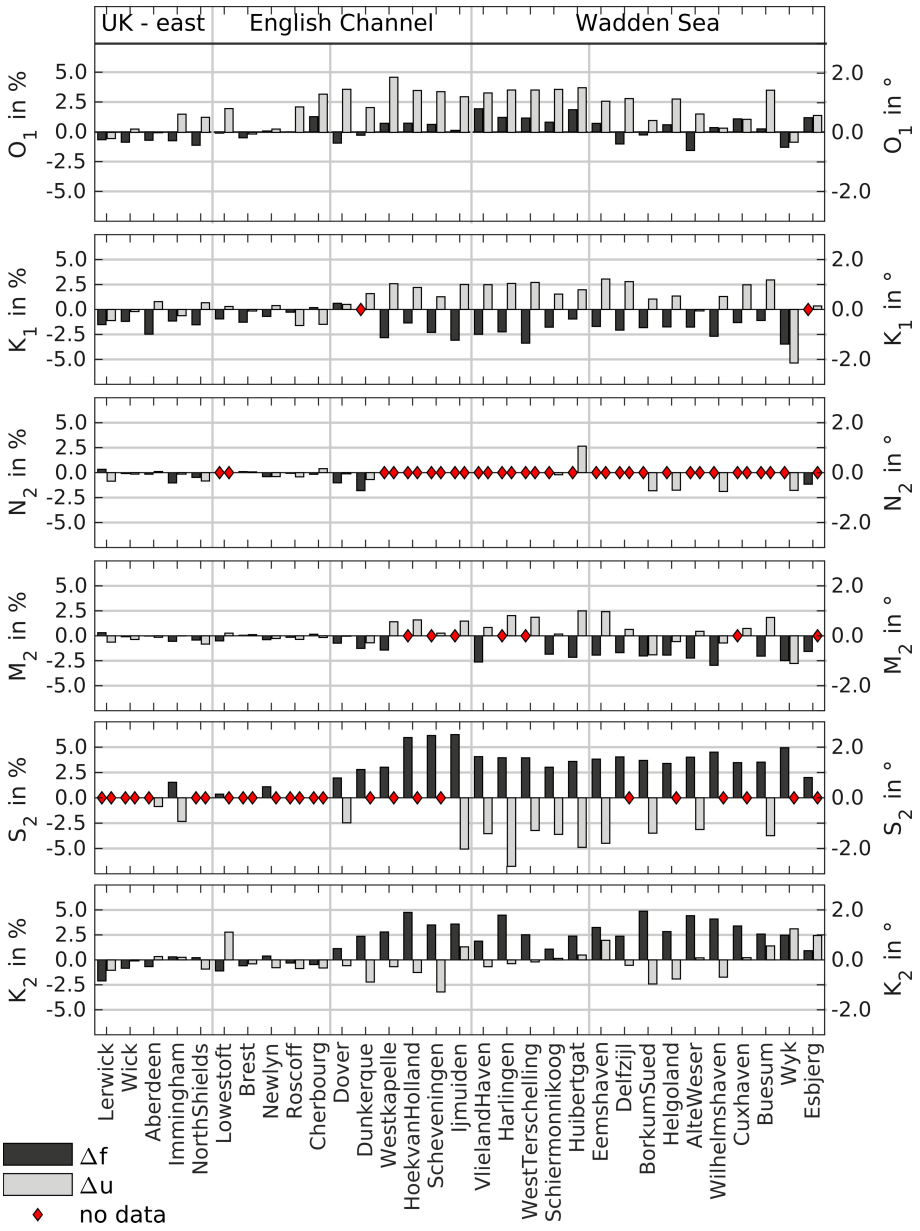

Figure 6: Differences between the fitted amplitude modulation in % (left y-axis, black) and phase lag in ° (right y-axis, gray) and the equilibrium nodal correction parameters (i.e. Table 1) for the constituents M_2, S_2, N_2, O_1, K_1 and K_2. Data points with an insufficient R^2 are marked with a red dot.

The amplitude modulation of O_1 is overestimated most in Vlieland Haven (1.9 %) and Huibertgat (1.9 %) in the Dutch Wadden Sea. The following stations show differences ranging from 0.7 % (Eemshaven) towards an underestimation of -1.6 % at Alte Weser in the German Wadden Sea. K_1's amplitude modulation is underestimated throughout all locations except for Cherbourg and Dover. At the east coast of the UK it is underestimated by -2.5 % in Aberdeen to -1.5 % in North Shields. The westerly stations Newlyn, Brest

and Roscoff underestimate K_1 by less than -0.7 %, while the maximum underestimation is reached in Westkapelle (-2.8 %), Ijmuiden (-3.1 %) and West Terschelling (-3.4 %). Though N_2 must be modulated by the nodal tide due to the laws of astronomy, its variation could only be detected until Cherbourg in the southern English Channel and at the UK east coast. Successfully fitted N_2 amplitude variation is underestimated slightly on the English east coast from Aberdeen (-0.1 %) to Immingham (-1.1 %). Gauges in the southern English Channel underestimate N_2's amplitude modulation by less by -0.4 % in Newlyn until -1.8 % in Dunkerque. The nodal component of the semidiurnal M_2 is underestimated consistently after the Dover-Calais narrowing in the English Channel. In Westkapelle, the M_2 modulation starts to be underestimated by -1.4 % and -0.7% in Dover. When moving further northeastwards the nodal amplitude modulation of M_2 diminishes into statistical insignificance until reaching the Dutch Wadden Sea. In Vlieland Haven, M_2 modulation is reduced by -2.6 %, although within the Wadden Sea itself, M_2 modulation is mostly reduced by -2.0 % (Vlieland Haven to Wyk). Harlingen, West-Terschelling and Cuxhaven did not meet the criterion for statistical significance. S_2 shows a similar behavior, as its amplitude is modulated between Dover (2.0 %) and Esbjerg (2.0 %), peaking near the S_2 amphidrome at Ijmuiden (6.2 %). In the Wadden Sea, S_2 is modulated consistently between Vlieland Haven (4.1 %) and Büsum (3.5 %). Contrarily, the nodal amplitude variation of K_2 is overestimated after the Dover-Calais narrowing by 1.1 % in Dover and 2.8 % in Westkapelle. The K_2 amplitude variation remains exaggerated by 4.8 % in Hoek van Holland, 1.9 % in Vlieland Haven, 2.4 % in Huibertgat, 4.4 % in Alte Weser and 2.6 % in Büsum within the Wadden Sea before reaching a smaller overestimation in Esbjerg of 0.9 %. Although, the phase lags of all constituents do not deviate more than $\pm 2.0\,^{\circ}$ at any location, they show consistent variance from their equilibrium modulation value u with an overestimation between 0.5 to $2.0\,^{\circ}$ of O_1, K_1, S_2 and M_2 for all gauges from Dunkerque to Büsum.

3.4 The Impact of Shallow Water Constituents

When tides travel from the open sea towards coastal waters, embayments or estuaries, energy dissipation through friction leads to the generation of new tidal constituents, which are called shallow water tides. They are related to larger parent constituents, which are astronomically predefined, e.g. M_2 or S_2. In other words, the generation of shallow water tides drains energy from parent constituents, which underlie the nodal tide modulation. Hence, it is not prudent to imply a connection between bottom friction on nodal modulation, especially because this has already been suspected in Feng et al. (2015) and Godin (1986). However, the quantity and amplitude of shallow water tides vary regionally, which is why the shallow water tide hypothesis above may not hold true for all coastal waters equally. As the underestimation of f for K_2 and O_1 in section 3.3 coincides with an overestimation of the nodal amplitude modulation of M_2, N_2 and S_2, we suspect interactions between the parent constituents through their shallow water tides to be the dominant driver for these deviations from the equilibrium tide in the North Sea.

To support the shallow water tide hypothesis, a harmonic analysis at representative gauges near the British east coast and in the Wadden Sea was carried out for M_2 and S_2's shallow water constituents. In Büsum (Wadden Sea), for example, 10 shallow water components with an amplitude larger than 3 cm were present in 2012 of which MSf, M_4, M_6, MU_2, MS_4, NU_2, $2MS_6$ and MN_4 are related to a lunar origin. If the constituents, which are either solar or lunar influenced and the meteorological tide MSf are ruled out, MS_4 and $2MS_6$ remain. Multiple, non-linear regression fitting (Equation 1) of MS_4 and $2MS_6$ has shown that, a clear nodal signal could not be extracted from these components at any of the locations presented in 3. However, significant amplitude differences of MS_4 and $2MS_6$ between the gauges do exist. If the M_2 to MS_4 or the M_2 to $2MS_6$ amplitude ratios, respectively, are calculated, large values coincide with S_2 modulation as demonstrated in Table 3.

Table 3: Ratios of significant shallow water components, which are created from S_2 and M_2 for representative gauges in the deeper North Sea (Brest, Lerwick, North Shields), the English Channel (Lowestoft) and the Wadden Sea (Vlieland Haven, Delfzijl, Büsum). $R^2 \geq 0.50$ indicates a successful fitting of nodal variation for S_2.

	$\frac{M_2}{MS_4}$ in -	$\frac{M_2}{2MS_6}$ in -	R^2 for S_2
Brest	0.016	0.008	0.010
Lerwick	0.021	0.021	0.171
North Shields	0.012	0.005	0.093
Lowestoft	0.061	0.061	0.771
Vlieland Haven	0.039	0.061	0.830
Delfzijl	0.090	0.050	0.606
Büsum	0.040	0.015	0.604

While the ratios do not exceed 0.021 in Brest, Lerwick, North Shields at the UK east coast, larger ratios are observed in Lowestoft (0.061), Vlieland Haven (0.061), Delfzijl (0.09) or Büsum (0.04). These larger ratios coincide with significant index of agreement values of $R^2 > 0.5$, showing a relationship between the modulation of S_2 and large shallow water tide amplitudes. An analog analysis for K_2 has shown additionally, that the overestimation of K_2 (see also Figure 6) coincides with large K_2 to either MK_4, $2MK_6$ or MKS_2 ratios.

3.5 Spatial Nodal Modulation

The amplitude modulation f and phase lag u has been shown to differ significantly from expected equilibrium conditions in measured tide records (i.e. Figure 6). Furthermore, the fitted nodal modulation shows regional tendencies, for example when the modulation of the M_2 in the Dutch side of the English Channel is reviewed. The nodal modulation corresponds to equilibrium values in Cherbourg, is overestimated near the Dover-Calais narrowing at Dunkerque / Dover, before diminishing into statistical insignificance in Westkapelle to Ijmuiden. Another example is the nodal amplitude variation of N_2, which has not produced any results between Westkapelle and Wyk due to statistical insignificance.

Therefore, we computed a complete spatial distribution of the amplitude and phase correction parameters for the North Sea with the numerical model from Section 2.4 in order to quantify the regional variation. As a consequence of the long time scale of 18.61 years a simulation would require a time period of roughly 19 years. For this reason, the model has only been applied for 10 months with the diurnal amplitude modulation and phase lag minima and maxima reached 5 months into the computation, as other solutions would be computationally expensive. The diurnal phase lag minimum is in October 2001, its maximum in February 2011, while the diurnal amplitude modulation minimum is in June 2006 and its maximum in October 2015, respectively (Pugh, 1987). The model is forced astronomically at the open boundaries by $f-u$ corrected, reanalyzed tidal constituents from the FES 2014b (Section 2.4). Meteorology has been deactivated and the bathymetry is not altered between each simulation. Model results have been interpolated from the unstructured computational grid on a regular 7.5 km grid before the harmonic analysis UTide without nodal correction has been applied. The spatial nodal modulation is then calculated through the absolute amplitude difference between 2006 and 2015, divided by their mean, and the phase lag is calculated by subtracting 2001 from 2011. The resulting values must be halved, as an amplitude is only half of the sinusoidal range.

3.5.1 Computed Nodal Modulation at Gauges

Before determining the spatial distribution of amplitude modulation f and phase lag u, the model results are compared to the analysis results from tide records in Section 3.3. The index of agreement (R^2) is applied for the observed and modeled (predicted) nodal satellite variation. To quantify the quality of the computed nodal variation, a mean absolute error (MAE) and a root mean square error (RMSE) are given in Table 4. The actual model validation is referred to in Section 2.4.

Table 4: Validation parameters for modeled and observed nodal satellite variation correction parameters f and u. MAE and RMSE are displayed in % and °, respectively, and R^2 dimensionless.

	Parameter	O_1	K_1	N_2	M_2	S_2	K_2
f	MAE	1.8	4.0	0.5	0.5	1.5	1.2
	RMSE	2.1	4.1	0.8	0.7	1.7	1.5
	R^2	0.12	0.00	0.55	0.79	0.76	0.53
u	MAE	0.7	0.8	0.5	0.5	0.7	0.6
	RMSE	0.9	0.9	0.7	0.6	0.8	0.8
	R^2	0.00	0.00	0.04	0.05	0.03	0.14

The validation of the computed amplitude modulation shows $R^2 > 0.5$ for the semidiurnal constituents N_2, M_2, S_2 and K_2, proving a linear dependency between observed and computed nodal modulation. The semidiurnal MAEs range between 0.5 and 1.5 % and the RMSEs between 0.7 to 1.5 %, respectively. The differences result from a weaker model response to amplitude modulation, especially for K_2 and S_2, though the prediction of over- or underestimation, of nodal modulation remains correct. The amplitude modulation of diurnal components K_1 and O_1, however demonstrates lower agreement to the predicted counterpart. The model produces an overestimation of K_1 by an MAE of 1.8 % for O_1 and 4.0 % for K_1. The larger error residuals result from an overestimation of nodal amplitude variation in the model. For K_1 especially, the model calculates an overestimation of the amplitude modulation, while observations have shown an underestimation from the equilibrium value. This holds true for O_1 as well, though prediction and observation display an overestimation of O_1s amplitude modulation with weak R^2 of 0.12. For the nodal phase lag, R^2 ranges between 0 for O_1 and 0.14 for K_2, which results from the models inability to reproduce a nodal phase variation, which differs from the equilibrium tide. Opposing to the fitting results from measurements, the model computes phase lags, which correlate with the equilibrium value for all constituents. This results in low R^2 for the phase lag as can be seen in Table 4.

3.5.2 Modeled Nodal Variation

The amplitude of a nodal constituent (left), its nodal amplitude modulation (middle) and its phase lag (right), as computed in the numerical model are shown in Figure 7. We will focus on the nodal modulation of M_2, N_2, K_2 and O_1 subsequently, as these constituents have shown strong regional tendencies. In the following, the index n denotes the nodal satellite of a constituent.

The largest nodal amplitude is observed for M_{2n} with more than 15 cm in the southern English Channel. The amplitude in the Wadden Sea ranges between 2 and 4 cm, while the Dutch west coast and the Danish north coast show amplitudes of ≤ 1 cm. M_2's nodal amplitude modulation corresponds with the equilibrium value in the southern English Channel and the UK east coast (3.7 %). It is underestimated on the Dutch side of the English Channel (1.5 to 2.0 %) and the eastern German Wadden Sea (2.0 to 3.0 %). The phase lag u of M_2 shows low deviations between -2.1 to -2.4 ° in the southern North Sea. The amplitude distribution of N_{2n} is similar to M_{2n} and K_{2n}, though the amplitude of N_{2n} is significantly lower with a maximum of $4cm$ in the southern English Channel and 0.5 to 1.2 cm in the Wadden Sea. N_{2n}'s amplitude is below 0.5 cm on the western Dutch coast, Northern Frisia in Germany and the Danish North Sea coast, indicating, why nodal amplitude modulation could not be derived from tide records at these locations. The deviation from the theoretical phase lag u tends to be underestimated between 1.1 and 2.5 ° for N_2. The amplitude distribution and magnitude of K_{2n} is again similar to M_{2n}, with maximum amplitudes of 15 cm in the southern English Channel. K_2's amplitude modulation is overestimated by 1.5 % in the English Channel and the Dutch Wadden Sea and by 3 % near the Dutch west coast. UK's east coast and the southern English Channel remain unaffected as seen previously for M_{2n} and N_{2n}. The phase lag of K_{2n} deviates less than 1.5 ° from its correction value u almost in the entire study area. O_{1n} has its maximum amplitude in the UK Moray Firth and Thames estuary at 3.8 cm and its amplitude is $\leq$ 1 cm at the Norwegian coast, the Danish northwest coast and the southern English Channel. The equilibrium tide nodal modulation is well represented near the model boundaries (≤ 0.5 %), before the model reveals an amplification of O_1 amplitude modulation at the English east coast (1.0%), the eastern English channel (1.5%), the Dutch west coast the Wadden Sea (2.5 %). The nodal phase lag u for O_{1n} shows small regional deviation with maximum differences in the English Channel near its amphidromy and in the Dutch and German Wadden Sea (1.0 °).

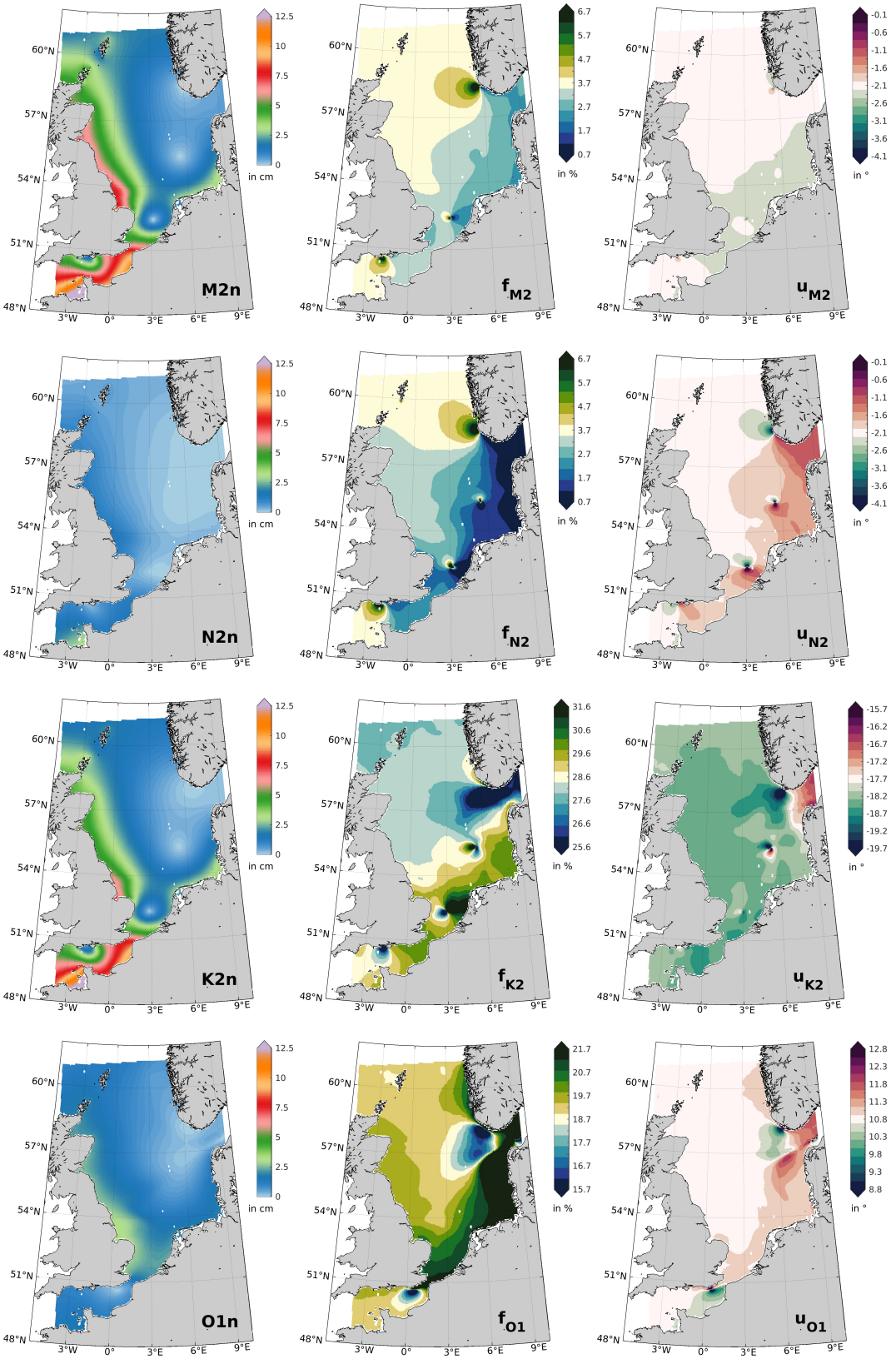

Figure 7: Spatial distribution of the nodal amplitude in *cm* (left), the nodal modulation f in % (middle) and the nodal phase lag u in ° (right) for the tidal constituents M_2, N_2, K_2 and O_1 as computed by the numerical model. The theoretical nodal modulation and phase lag values from the equilibrium tide theory are placed in the center of the colorbar for the f (middle) and u (right) plots, with a range of ±3 % and ±2 °, respectively.

4 Discussion

This study has shown, based on measured tide records, that the nodal correction parameters f (amplitude) and u (phase) for lunar tidal constituents in harmonic analysis do not always follow the equilibrium tide theory, opposing to the statements in Trupin and Wahr (1990). This analysis corroborates previous results, whom discussed the nodal correction parameters based on the equilibrium tide assumption (e.g. Cherniawsky et al. (2010); Feng et al. (2015); Godin (1986); Shaw and Tsimplis (2010) to name only a few) and extends the current analysis methods for nodal tide estimation by introducing a multiple, non-linear fitting approach for tidal constituents. Unlike the commonly applied quantile method (Woodworth & Blackman, 2004), the application of multiple, non-linear regression to annually calculated, tidal constituents accounts for the accelerated change in semidiurnal tides (Baart et al., 2012; Müller, 2011) and is applicable for tide records with a duration of more than 19 years in the North Sea.

In contrast to previous research (Godin, 1986; Shaw & Tsimplis, 2010), the nodal modulation of constituents does not follow the equilibrium tide theory strictly, as O_1 and K_2 are underestimated in the English Channel and the Wadden Sea (see Figure 6). M_2's nodal modulation agrees well with previous findings (Feng et al., 2015; Ku et al., 1985; Woodworth et al., 1991), as it is reduced in the friction dominated areas of the study site such as the Dutch east coast and the Wadden Sea. Nevertheless, the fitting of N_2 in the same areas remained inconclusive, which was associated with the friction induced generation of shallow water tides and third order disturbances (Godin, 1986). The amplitude modulation of the constituent K_1 differs from the other semidiurnal results, as nodal modulation is already reduced in the Northern Atlantic (i.e. Lerwick, Newly, Brest in Figure 6), though its amplitude modulation is consistently reduced at the Dutch east coast and the Wadden Sea. These findings disagree with Godin (1986), who stated that the nodal correction of K_1, K_2 and O_1 is appropriate in any case. Moreover, the agreement found in the Mediterranean Seas (Shaw & Tsimplis, 2010) can only be observed outside the English Channel and the Wadden Sea. However, the interpretation of the results of this study must consider, that the amplitude of the nodal satellites is often smaller than 5 cm in the North Sea. Therefore, small error margins resulting e.g. from the 95 % confidence interval in harmonic analysis may lead to under- or overestimation when reviewing small amplitudes. The amplitude of $K_{1,n}$ for example rarely exceeds 1 cm in the entire study area. The underestimation of K_2 and O_1 coincided with an overestimation of M_2, N_2 and a nodal modulation of the solar constituent S_2. For this reason, we suspect interactions within these constituents and their shallow water tides must be responsible. Furthermore, as an overestimated nodal amplitude modulation for K_2 has not yet been documented in literature, other non-linear effects such as diffraction, reflection or refraction may be present. The deviation from the equilibrium for the nodal phase lag from tide records was be considered negligible for all constituents, as the difference rarely exceeds 2.5 °, which would correspond to approximately 5 minutes for the M_2.

In order to fortify the hypothesis, that shallow water effects cause the deviation from the equilibrium tide, a spatial distribution of nodal amplitude modulation f and phase lag u was determined by numerical modeling to distinctively identify affected regions as suggested by Woodworth (2012). The modeling approach has shown considerable skill for the amplitude modulation of semidiurnal constituents, but is less suitable concerning the diurnal components K_1 and O_1 and the nodal phase lag of all constituents. We find certain limitations to arise from the accuracy of the numerical model itself, which has been validated to an order of centimeters and minutes (Bundesanstalt für Wasserbau et al., 2019b) and the harmonic analyses timespan, which differs marginally by 2 months between the model and the tide records. The poor agreement concerning the phase lag agreement could be related to the natural bathymetry changes in the North Sea between the years 2001 to 2015, but these are not included in the model. The link between tidal constituents and bathymetry changes in the Wadden Sea is well established (Jacob et al., 2016; Rasquin et al., 2020), which would suggest, that the deviation of the nodal phase lag in tide records originates from morphodynamic changes.

Still, the question arises, why the diurnal constituent representation did not achieve the same quality as the semidiurnals in the numerical model. Nevertheless, the model results have revealed regionally deviating amplitude modulation in areas with strong friction such as the English Channel or the Wadden Sea. Since meteorological and thus seasonal influences were neglected in the modeling approach, friction remains as the only major possible cause for shifts in nodal modulation. Friction is induced by the shallow water of the continental shelf and complex basin geometry, which becomes increasingly relevant in the English Channel and in the Wadden Sea. Therefore, we conclude, similar to Feng et al. (2015) a friction induced generation of shallow water tides in the inner North Sea, which leads to a reduced amplitude modulation of M_2 and N_2. However, the amplitude modulation of K_2, S_2 and O_1 is also affected, which partially disagrees with the results from the Chinese Seas (Feng et al., 2015), as K_2s modulation is significantly underestimated while O_1 is overestimated in the North Sea. Since K_2s and O_1s deviation coincide with the underestimation of M_2 and N_2, we again suspect the energy transfer towards shallow water constituents to be responsible. The shallow water tide hypothesis shows most obvious in the modulation of the solar constituent S_2, which should not be affected by the nodal tide whatsoever. In fact, every time the modulation of M_2 was reduced, the variation of K_2 and S_2 became enhanced. We have shown, that the modulation of S_2 links to high amplitudes of the shallow water tides MS_4 and $2MS_6$ (i.e. Table 3), which for MS_4 has also been shown in the Chinese Seas (Feng et al., 2015). An analog harmonic analysis for the parent constituent K_2 has shown a similar relationship to its shallow water components MK_4, $2MK_6$ or MKS_2. Even though the relationship between shallow water tides and the deviation of the nodal amplitude modulation has been proven in this study, more work is required in order to quantify the influence of shallow water tides on the nodal tide, specifically. Other non-linear effects, such as shoaling, reflection, refraction or diffraction may also disrupt the nodal modulation, especially in the English Channel.

5 Summary and conclusion

In sea level science, an accurate estimation of low frequency tides, such as the lunar 18.61 year nodal tidal cycle is crucial, as the nodal amplitude can be up to 30 cm (Peng et al., 2019). Even though different methods, such as the quantile method (Woodworth & Blackman, 2004), have been used to quantify a nodal amplitude and phase lag from tide records, an accurate approximation is not yet consistently applicable at any geographical location. Nodal modulation is defined as the correction of lunar tidal constituents from harmonic tide analysis through the f (amplitude) and u (phase) correction parameters, which are derived from the equilibrium tide theory (Pugh, 1987). Past studies have shown these correction parameters to be accurate (Godin, 1986; Shaw & Tsimplis, 2010; Trupin & Wahr, 1990), overestimated (Feng et al., 2015) or underestimated (Cherniawsky et al., 2010) depending on the geographical location and analysis method. For this reason, the correction parameters are calculated and compared to the equilibrium approach at various tide records in the North Sea and North Atlantic region to find an approach, which accurately extracts the nodal tide from gauge records. Furthermore, a numerical model is deployed at the diurnal minimum and maximum of nodal amplitude modulation and phase lag to provide spatial information in between the gauge network at the North Sea. The overall aim is to develop and validate a method to extract the nodal signal from tide records and to supply large-scale information on the nodal modulation in shelf seas, such as the North Sea, as sea level sciences rely on accurate assumptions of the nodal cycle.

A multiple, non-linear regression analysis of annual tidal constituents at North Sea gauges was chosen to approximate nodal amplitude and phase modulation. The results have shown, that the amplitude correction parameter f is significantly overestimated for M_2, N_2 and underestimated for K_1, K_2, O_1 in shallow, friction dominated parts of the North Sea, although the calculated phase lag coincides well with deviations of less than 2.0 °. Additionally, the solar constituent S_2 was shown to be modulated regionally in the Northern English Channel and the Wadden Sea. We support the hypothesis from literature (Feng et al., 2015; Pugh, 1987), whom state that energy transfer from M_2 and S_2 towards shallow water tides such as MS_4 or $2MS_6$ leads to S_2's modulation. Shallow water effects also influence other diurnal and semidiurnal constituents such as O_1, K_1, K_2 or N_2, though more research is needed on this subject. We could not identify the dominant process behind the underestimation of amplitude modulation f for O_1 and K_2, as well as the overall overestimation of K_1 as similar effects have not yet been documented in literature. A link between K_2 and the shallow water constituents MK_4, $2MK_6$ or MKS_2, however, was established. A larger scale could provide more insight about the processes at play, though we suspect shallow water dynamics to be responsible for the overestimation of O_1 or K_2.

The numerical modeling studies have confirmed, that friction affected areas, such as the English Channel or the Wadden Sea, reduce the nodal amplitude modulation of M_2, while the variation of O_1, S_2 and K_2 is enhanced. The distribution of f is hereby inhomogeneous, as regional and local differences are present due to the variety of generated shallow water tides. An analysis of shallow water constituents of the tide record at Büsum, for example, has revealed a larger M_2 to MS_4 or $2MS_6$ ratio when the modulation of S_2 became significant. Thus, we concluded that the current $f-u$ correction should only be applied, whenever the influence of shallow water tides is negligible, as they influence the nodal modulation of lunar constituents and S_2. The application of u can hereby be regarded reasonable due to low deviations of less than ±2.5 °. It must be noted that these recommendations do depend on the field of application and the user-desired degree of accuracy.

Despite the wide acceptance of the $f - u$ nodal correction methodology, it may significantly deviate from the equilibrium in friction affected areas. Additionally, the $f-u$ correction does not consider the modulation of S_2. Therefore, the $f-u$ correction parameters must be determined appropriately and if necessary, corrected. This process is simplified with the non-linear, multiple regression of tidal constituents presented in this study, which enables the calculation of accurate f and u correction values. Future work is recommended

towards the extension of these regional results to a global scale. This can be performed numerically by global modeling scenarios or analytically by non-linear, multiple regression analysis of satellite altimetry data. The resulting product would be a globally varying data set providing appropriate f and u correction factors. A correction layer, which includes non-lunar, yet modulated constituents such as S_2, could stand behalf of the general correction formulation for a more accurate, spatially varying nodal modulation correction. Future work is also recommended towards quantifying the effect of shallow water tides on the nodal satellite variation, especially as many gauges are located in complex coastal or estuarine environments in practice. This would aid sea level science, as the correction of tide records for nodal modulation would be more accurate and help to understand yet unexplained phenomena.

Acknowledgments

We thank the German Federal Ministry of Transport (BMVI) for funding the mFUND project EasyGSH-DB (funding no. 19F2004A), which has made this research possible. Also, we would like to thank the suppliers of tide records from Germany (German Waterways and Shipping Administration (WSV) in cooperation with the German Federal Institute of Hydrology (BfG), France (Shom), the UK (BODC) and the Netherlands (Rijkwaterstaat). Tide records can be retrieved from `https://data.shom.fr/`, `https://www.bodc.ac.uk/data/` and `https://waterinfo.rws.nl/`.

RH would also like to thank his friend Dirk Hagemann personally for in depth discussions about advanced signal processing and analysis.

References

Amin, M. (1985). Temporal variations of tides on the west coast of great britain. *Geophysical Journal International*, *82*(2), 279–299. doi: \url{10.1111/j.1365-246X.1985.tb05138.x}

Amin, M. (1993). Changing mean sea level and tidal constants on the west coast of australia. *Marine and Freshwater Research*, *44*(6), 911. doi: \url{10.1071/MF9930911}

Baart, F., van Gelder, P. H. A. J. M., de Ronde, J., van Koningsveld, M., & Wouters, B. (2012). The effect of the 18.6-year lunar nodal cycle on regional sea-level rise estimates. *Journal of Coastal Research*, *280*, 511–516. doi: \url{10.2112/JCOASTRES-D-11-00169.1}

Bradley, J. (1728). An account of a new discovered motion of the fixed stars. *Philosophical Transactions of the Royal Society of London*, *35*(406), 637–661. doi: \url{10.1098/rstl.1727.0064}

Bundesanstalt für Wasserbau, Hagen, R., Freund, J., Plüß, A., & Ihde, R. (2019a). *Jahreskennblatt easygsh-db 2015. kurzfassung der validierung: Untrim2 - sedimorph - unk.* Bundesanstalt für Wasserbau. doi: \url{10.18451/k2{\textunderscore}easygsh{\textunderscore}jkbl{\textunderscore}2015}

Bundesanstalt für Wasserbau, Hagen, R., Freund, J., Plüß, A., & Ihde, R. (2019b). *Validierungsdokument easygsh-db nordseemodell. teil: Untrim2 – sedimorph – unk.* Bundesanstalt für Wasserbau. doi: \url{10.18451/k2{\textunderscore}easygsh{\textunderscore}1}

Casulli, V. (2009). A high-resolution wetting and drying algorithm for free-surface hydrodynamics. *International Journal for Numerical Methods in Fluids*, *60*(4), 391–408. doi: \url{10.1002/fld.1896}

Casulli, V., & Walters, R. A. (2000). An unstructured grid, three-dimensional model based on the shallow water equations. *International Journal for Numerical Methods in Fluids*, *32*(3), 331–348. doi: \url{10.1002/(SICI)1097-0363(20000215)32:3{\textless}331::AID-FLD941{\textgreater}3.0.CO;2-C}

Cherniawsky, J. Y., Foreman, M. G., Kuh Kang, S., Scharroo, R., & Eert, A. J. (2010). 18.6-year lunar nodal tides from altimeter data. *Continental Shelf Research*, *30*(6), 575–587. doi: \url{10.1016/j.csr.2009.10.002}

Codiga, D. L. (2011). *Unified tidal analysis and prediction using the utide matlab functions.* Graduate School of Oceanography, University of Rhode Island. doi: \url{10.13140/RG.2.1.3761.2008}

Doodson, A. T. (1921). The harmonic development of the tide-generating potential. *Proceedings of the Royal Society A: Mathematical, Physical and Engineering Sciences*, *100*(704), 305–329. doi: \url{10.1098/rspa.1921.0088}

Doodson, A. T. (1928). The analysis of tidal observations. *Philosophical Transactions of the Royal Society A: Mathematical, Physical and Engineering Sciences*, *227*(647-658), 223–279. doi: \url{10.1098/rsta.1928.0006}

EMODnet Bathymetry Consortium. (2016). *Emodnet digital bathymetry (dtm 2016).* Author. doi: \url{10.12770/c7b53704-999d-4721-b1a3-04ec60c87238}

Feng, X., Tsimplis, M. N., & Woodworth, P. L. (2015). Nodal variations and long-term changes in the main tides on the coasts of china. *Journal of Geophysical Research: Oceans*, *120*(2), 1215–1232. doi: \url{10.1002/2014JC010312}

Foreman, M. G. G., Cherniawsky, J. Y., & Ballantyne, V. A. (2009). Versatile harmonic tidal analysis: Improvements and applications. *Journal of Atmospheric and Oceanic Technology*, *26*(4), 806–817. doi: \url{10.1175/2008JTECHO615.1}

Godin, G. (1972). The analysis of tides. *Liverpool University Press*, 264 pp.

Godin, G. (1986). The use of nodal corrections in the calculation of harmonic constants. *International Hydrographic Review*(63 (2)).

Gräwe, U., Burchard, H., Müller, M., & Schuttelaars, H. M. (2014). Seasonal variability in m 2 and m 4 tidal constituents and its implications for the

coastal residual sediment transport. *Geophysical Research Letters*, *41*(15), 5563–5570. doi: \url{10.1002/2014GL060517}

Haigh, I. D., Eliot, M., & Pattiaratchi, C. (2011). Global influences of the 18.61 year nodal cycle and 8.85 year cycle of lunar perigee on high tidal levels. *Journal of Geophysical Research*, *116*(C6), 25249. doi: \url{10.1029/2010JC006645}

Haigh, I. D., Pickering, M. D., Green, J. M., Arbic, B. K., Arns, A., Dangendorf, S., ... Woodworth, P. L. (2019). The tides they are a–changin': A comprehensive review of past and future non–astronomical changes in tides, their driving mechanisms and future implications. *Reviews of Geophysics*. doi: \url{10.1029/2018RG000636}

Hansen, J. M., Aagaard, T., & Kuijpers, A. (2015). Sea-level forcing by synchronization of 56- and 74-year oscillations with the moon's nodal tide on the northwest european shelf (eastern north sea to central baltic sea). *Journal of Coastal Research*, *315*, 1041–1056. doi: \url{10.2112/JCOASTRES-D-14-00204.1}

Houston, J. R., & Dean, R. G. (2011). Accounting for the nodal tide to improve estimates of sea level acceleration. *Journal of Coastal Research*, *276*, 801–807. doi: \url{10.2112/JCOASTRES-D-11-00045.1}

Jacob, B., Stanev, E. V., & Zhang, Y. J. (2016). Local and remote response of the north sea dynamics to morphodynamic changes in the wadden sea. *Ocean Dynamics*, *66*(5), 671–690. doi: \url{10.1007/s10236-016-0949-8}

Jay, D. A., Leffler, K., Diefenderfer, H. L., & Borde, A. B. (2015). Tidal-fluvial and estuarine processes in the lower columbia river: I. along-channel water level variations, pacific ocean to bonneville dam. *Estuaries and Coasts*, *38*(2), 415–433. doi: \url{10.1007/s12237-014-9819-0}

Jensen, J., Mügge, H. E., & Schönfeld, W. (1992). Analyse der wasserstandsentwicklung und tidedynamik in der deutschen bucht: Abschlussbericht zum kfki-projekt - wasserstandsentwicklung in der deutschen bucht. *Die Küste*(53), 211–275. Retrieved 01.08.2019, from `\url{https://hdl.handle.net/20.500.11970/101341}`

Jensen, J., Mügge, H. E., & Visscher, G. (1988). Untersuchungen zur wasserstandsentwicklung in der deutschen bucht: Zwischenbericht zum kfki-projekt - wasserstandsentwicklung in der deutschen bucht. *Die Küste*(47), 135–161. Retrieved from `\url{https://hdl.handle.net/20.500.11970/101279}`

Ku, L. F., Greenberg, D. A., Garrett, C. J., & Dobson, F. W. (1985). Nodal modulation of the lunar semidiurnal tide in the bay of fundy and gulf of maine. *Science (New York, N.Y.)*, *230*(4721), 69–71. doi: \url{10.1126/science.230.4721.69}

Menéndez, M., & Woodworth, P. L. (2010). Changes in extreme high water levels based on a quasi-global tide-gauge data set. *Journal of Geophysical Research*, *115*(C10), 267. doi: \url{10.1029/2009JC005997}

Müller, M. (2011). Rapid change in semi-diurnal tides in the north atlantic since 1980. *Geophysical Research Letters*, *38*(11), n/a-n/a. doi: \url{10.1029/2011GL047312}

Müller, M., Cherniawsky, J. Y., Foreman, M. G. G., & von Storch, J.-S. (2014). Seasonal variation of the m 2 tide. *Ocean Dynamics*, *64*(2), 159–177. doi: \url{10.1007/s10236-013-0679-0}

Peng, D., Hill, E. M., Meltzner, A. J., & Switzer, A. D. (2019). Tide gauge records show that the 18.61–year nodal tidal cycle can change high water levels by up to 30 cm. *Journal of Geophysical Research: Oceans*, *124*(1), 736–749. doi: \url{10.1029/2018JC014695}

Proudman, J. (1960). The condition that a long-period tide shall follow the equilibrium-law. *Geophysical Journal International*, *3*(2), 244–249. doi: \url{10.1111/j.1365-246X.1960.tb00392.x}

Pugh, D. T. (1987). *Tides, surges and mean sea level*. Chichester: Wiley.

Rasquin, C., Seiffert, R., Wachler, B., & Winkel, N. (2020). The significance of coastal bathymetry representation for modelling the tidal response to mean sea level rise in the german bight. *Ocean Science*, *16*(1), 31–44. doi: \url{10.5194/os-16-31-2020}

Ray, R. D. (2006). Secular changes of the m tide in the gulf of maine. *Continental Shelf Research*, *26*(3), 422–427. doi: \url{10.1016/j.csr.2005.12.005}

Rossiter, J. R. (1967). An analysis of annual sea level variations in european waters. *Geophysical Journal International*, *12*(3), 259–299. doi: \url{10.1111/j.1365-246X.1967.tb03121.x}

Sehili, A., Lang, G., & Lippert, C. (2014). High-resolution subgrid models: Background, grid generation, and implementation. *Ocean Dynamics*, *64*(4), 519–535. doi: \url{10.1007/s10236-014-0693-x}

Shaw, A., & Tsimplis, M. N. (2010). The 18.6yr nodal modulation in the tides of southern european coasts. *Continental Shelf Research*, *30*(2), 138–151. doi: \url{10.1016/j.csr.2009.10.006}

Sündermann, J., & Pohlmann, T. (2011). A brief analysis of north sea physics. *Oceanologia*, *53*(3), 663–689. doi: \url{10.5697/oc.53-3.663}

Trupin, A., & Wahr, J. (1990). Spectroscopic analysis of global tide gauge sea level data. *Geophysical Journal International*, *100*(3), 441–453. doi: \url{10.1111/j.1365-246X.1990.tb00697.x}

Woodworth, P. L. (2012). A note on the nodal tide in sea level records. *Journal of Coastal Research*, *280*, 316–323. doi: \url{10.2112/JCOASTRES-D-11A-00023.1}

Woodworth, P. L., & Blackman, D. L. (2004). Evidence for systematic changes in extreme high waters since the mid-1970s. *Journal of Climate*, *17*(6), 1190–1197. doi: \url{10.1175/1520-0442(2004)017{\textless}1190:EFSCIE{\textgreater}2.0.CO;2}

Woodworth, P. L., Shaw, S. M., & Blackman, D. L. (1991). Secular trends in mean tidal range around the british isles and along the adjacent european coastline. *Geophysical Journal International*, *104*(3), 593–609. doi: \url{10.1111/j.1365-246X.1991.tb05704.x}